Reexamination of phenomenological two-photon exchange corrections to the proton form factors and $e^{\pm}p$ scattering

I. A. Qattan,[1] A. Alsaad,[2] and J. Arrington[3]

[1]*Khalifa University of Science, Technology and Research, Department of Physics, P.O. Box 573, Sharjah, U.A.E*

[2]*Jordan University of Science and Technology, Department of Physical Sciences, P.O. Box 3030, Irbid 22110, Jordan*

[3]*Physics Division, Argonne National Laboratory, Argonne, Illinois, 60439, USA*

(Dated: September 8, 2011)

We extract the two-photon exchange (TPE) contributions to electron–proton elastic scattering using two parametrizations and compare the results to different phenomenological extractions and direct calculations of the TPE effects. We find that many of the extractions give similar results, and highlight the common assumptions and the impact of not including such assumptions. We provide a simple parametrization of the TPE contribution to the unpolarized cross section, along with an estimate of the fit uncertainties and the uncertainties associated with the assumptions made in the extraction. We look at the contributions as extracted from various e–p elastic scattering observables, and make predictions for ratio $R^{e^+e^-}$ of positron-proton to electron-proton elastic scattering cross sections.

PACS numbers: 25.30.Bf, 13.40.Gp, 14.20.Dh

I. INTRODUCTION

Electron scattering is a powerful technique used to reveal the underlying structure of the nucleon. This is because the electron is a point-like, structureless particle. This makes it an ideal probe of the target, as the cross section represents only known couplings and the (unknown) structure of the target. In elastic electron scattering, the incident electron is scatters off a nucleon target through the exchange of a virtual photon γ^*, and the structure of the target nucleon appears through two Sachs [1] electromagnetic form factors, G_{Ep} and G_{Mp}, which measure the deviation of the scattering from that for a point-like spin-1/2 target. As Q^2, the four-momentum squared of the virtual photon, increases the scattering becomes more sensitive to the small scale internal structure of the target.

Utilizing electron scattering, there are two methods used to extract the proton's form factors. The first is the Rosenbluth or Longitudinal-Transverse (LT) separation method [2], which uses measurements of the unpolarized cross section, and the second is the polarization transfer or polarized target (PT) method [3], which requires measurement of the spin-dependent cross section. In the Rosenbluth separation method, the reduced cross section σ_R is defined in the one-photon exchange (OPE) approximation as

$$\sigma_R = G_{Mp}^2(Q^2) + \frac{\varepsilon}{\tau} G_{Ep}^2(Q^2), \tag{1}$$

where $\tau = Q^2/4M_p^2$, M_p is the mass of the proton, and ε is the virtual photon longitudinal polarization parameter, defined as $\varepsilon^{-1} = \left[1 + 2(1+\tau)\tan^2(\frac{\theta_e}{2})\right]$, where θ_e is the scattering angle of the electron. For a fixed Q^2 value, the reduced cross section σ_R is measured at several ε points, and a linear fit of σ_R to ε gives $\tau G_{Mp}^2(Q^2)$ as the intercept and $G_{Ep}^2(Q^2)$ as the slope.

In the recoil polarization method, a beam of longitudinally polarized electrons scatters elastically from unpolarized proton target. The electrons transfer their polarization to the unpolarized protons. By simultaneously measuring the transverse, P_t, and longitudinal, P_l, polarization components of the recoil proton, one can determine the ratio $\mu_p G_{Ep}/G_{Mp}$ in the OPE [3–5]

$$\frac{G_{Ep}}{G_{Mp}} = -\frac{P_t}{P_l}\frac{(E+E')}{2M_p}\tan(\frac{\theta_e}{2}), \tag{2}$$

where E and E' are the initial and final energy of the incident electron, respectively. The ratio can be extracted in a similar fashion using polarized beams and targets by measuring the asymmetry for two different spin directions [6, 7].

The two methods yield significantly and strikingly different results in the region $Q^2 \geq 1.0$ (GeV/c)^2 with values of $\mu_p G_{Ep}/G_{Mp}$ differing almost by a factor of three at high Q^2. In the LT separation method, the ratio shows approximate form factor scaling, $\mu_p G_{Ep}/G_{Mp} \approx 1$, with some fluctuation at high Q^2 points. On the other hand, the recoil polarization method yields a ratio that decreases with increasing Q^2. The ratio is well parametrized [8] as:

$$\frac{\mu_p G_{Ep}}{G_{Mp}} = \mu_p R = 1 - 0.13(Q^2 - 0.04). \tag{3}$$

To reconcile the ratios, several studies suggested that missing higher order radiative corrections to the electron-proton elastic scattering cross sections can explain the discrepancy. In particular, studies focused on the role of the two-photon exchange (TPE) effect in resolving the discrepancy. The TPE effect was studied extensively both theoretically [9–14] and phenomenologically [15–23]. An extensive review of the role of the TPE effect in electron-proton scattering can be found in [24, 25].

II. TWO-PHOTON-EXCHANGE AND THE $e^{\pm}p$ CROSS SECTION SCATTERING RATIO

The interference of the OPE and TPE amplitudes represents the leading TPE correction to the electron-proton elastic scattering cross section. However, the recoil polarization data were confirmed experimentally to be essentially independent of ε [26]. We account for the TPE contribution to σ_R simply by adding the real function $F(Q^2,\varepsilon)$ to the Born reduced cross section:

$$\sigma_R = G_{Mp}^2\Big(1+\frac{\varepsilon}{\tau}R^2\Big) + F(Q^2,\varepsilon), \tag{4}$$

where $R = G_{Ep}/G_{Mp}$ is the recoil polarization ratio Eq. (3). The function $F(Q^2,\varepsilon)$ changes sign depending on the charge of the projectile (electron or positron). Therefore, $F(Q^2,\varepsilon)$ will have an opposite sign for electron-proton and positron-proton scattering cross section and any deviation of the ratio $R^{e^+e^-}(Q^2,\varepsilon)$ defined as

$$R^{e^+e^-}(Q^2,\varepsilon) = \frac{\sigma(e^+p\ \to e^+p)}{\sigma(e^-p\ \to e^-p)}, \tag{5}$$

from unity will be direct evidence for the TPE effect, and will therefore provide a direct way to determine its magnitude. The ratio $R^{e^+e^-}$ can be expressed as $R^{e^+e^-} \approx 1 + 4\Re(A_{2\gamma})/A_{1\gamma}$, with $A_{1\gamma}$ and $A_{2\gamma}$ being the OPE and TPE amplitudes [27], respectively. Here $\Re$ stands for the real part. On the other hand, the modification to the electron cross section is $\approx 1-2\Re(A_{2\gamma})/A_{1\gamma}$. Clearly, any change in the electron cross section will have almost twice the change in the ratio $R^{e^+e^-}$ but with the opposite sign. We will extract $R^{e^+e^-}$ based on our extraction of the TPE contributions, and also compare the results to other phenomenological extractions of the TPE contributions, comparing the 2γ corrections to σ_R and discussing the impact of the assumptions made in these analyses.

Recently, several theoretical studies estimated the function $F(Q^2,\varepsilon)$ [9–14]. Experimentally, studies focused on searching for nonlinearities in σ_R [16–18, 28] and phenomenologically by reanalyzing the experimental data using a proposed parametrization of the TPE contribution [15, 16, 18–23]. We present a summary of the results which we will examine in detail in this work.

Guichon and Vanderhaeghen [15] expressed the hadronic vertex function in terms of three independent complex amplitudes (generalized form factors) which depend on both Q^2 and ε: $\tilde{G}_{Ep}(\varepsilon,Q^2)$, $\tilde{G}_{Mp}(\varepsilon,Q^2)$, and $\tilde{F}_3(\varepsilon,Q^2)$. These generalized form factors can be broken into the usual Born (OPE) and the TPE contributions as: $\tilde{G}_{Ep,Mp}(\varepsilon,Q^2) = G_{Ep,Mp}(Q^2) + \Delta G_{Ep,Mp}(\varepsilon,Q^2)$ with $Y_{2\gamma}(\nu,Q^2)$ defined as $\Re\Big(\frac{\nu\tilde{F}_3}{M_p^2|\tilde{G}_{Mp}|}\Big)$, where $\Re$ stands for the real part, and $\nu = M_p^2\sqrt{(1+\varepsilon)/(1-\varepsilon)}\sqrt{\tau(1+\tau)}$. The reduced cross section is expressed in terms of these amplitudes as

$$\sigma_R = |\tilde{G}_{Mp}|^2\left[1+\frac{\varepsilon}{\tau}\frac{|\tilde{G}_{Ep}|^2}{|\tilde{G}_{Mp}|^2}+2\varepsilon\left(1+\frac{|\tilde{G}_{Ep}|}{\tau|\tilde{G}_{Mp}|}\right)Y_{2\gamma}\right]. \tag{6}$$

They demonstrated that small TPE contributions could significantly modify the extraction of the form factor ratio from the Rosenbluth separation, while having relatively little impact on the polarization transfer data. They also provided an estimate of the TPE amplitudes, based on the assumption that the entire contribution comes from the $Y_{2\gamma}(\nu,Q^2)$ term, parametrized so as to yield a correction to σ_R that is proportional to ε. This yields a small reduction in G_{Ep} as extracted from the polarization measurement, and a significant reduction in the Rosenbluth extraction of G_{Ep}, such that it becomes consistent with the corrected polarization results. In this work, G_{Mp} is unaffected by the TPE contributions.

Based on the framework of [15], Arrington [19] performed a global analysis where he extracted the TPE amplitudes $\Delta G_{Ep,Mp}$ and $Y_{2\gamma}$. He assumed that the amplitudes were ε-independent and took $\Delta G_{Ep} = 0$. Values for $Y_{2\gamma}(Q^2)$ were extracted from the difference between polarization and Rosenbluth measurements, taking into account the uncertainties in both data sets. Based on the high-ε constraints from the comparison of positron and electron scattering [29] the amplitude ΔG_{Mp} was determined by requiring that its contribution to σ_R at $\varepsilon = 1$ cancelled the contribution of $Y_{2\gamma}$. The extracted TPE amplitudes and their estimated uncertainties are then parametrized as a function of Q^2, and used to apply TPE corrections to the form factors obtained from a global Rosenbluth analysis [30] and the new recoil polarization data. Throughout this text, we will refer to the fit to the uncorrected Rosenbluth form factors obtained in Ref. [30] as the Arrington σ_R Fit, and to those corrected using the extracted TPE amplitudes as the Arrington $Y_{2\gamma}$ Fit [19].

In both of these analysis, there is not enough information to fully constrain the amplitudes, and so assumptions have to be made about the relative importance and the ε-dependence of the three TPE amplitudes. Common to these analyses are the assumption that the correction is close to linear in ε, as no non-linearities have been observed [16–18, 28]. If one also neglects the TPE correction to the polarization data, which is significantly smaller at high Q^2, then it is not necessary to work in terms of the polarization amplitude, and one can simply parametrize the TPE contributions to the reduced cross section, taking a linear (or nearly linear) ε dependence.

Alberico *et al.* [31] performed a global extraction of the proton form factors and TPE contributions, based on one of the parametrizations of the TPE contributions from Chen *et al.* [18]:

$$\sigma_R = G_{Mp}^2\Big(1+\frac{\varepsilon}{\tau}R^2\Big) + A(Q^2)y + B(Q^2)y^3, \tag{7}$$

where $y = \sqrt{(1-\varepsilon)/(1+\varepsilon)}$, $A(Q^2)=\alpha G_D^2(Q^2)$, $B(Q^2)=\beta G_D^2(Q^2)$ and $G_D(Q^2) = [1 +$

$Q^2/(0.71(\mathrm{GeV/c})^2)]^{-2}$ is the dipole form factor parametrization. Note that Chen *et al* performed such an extraction, but analyzed only the data of Ref. [32]. Alberico *et al* extract the form factors and the parameters α and β in two different ways. In the first fit, referred to throughout this text as ABGG Fit 1, the polarization transfer data was used to fix the ratio $R(Q^2) = \mu_p G_{Ep}/G_{Mp} = 1.022 - 0.13Q^2$ and G_{Mp} and the TPE contribution from Eq. (7) were determined in a global fit to world's cross section data. G_{Mp} was parametrized using the functional form from Kelly [33]:

$$\frac{G_{Mp}(Q^2)}{\mu_p} = \frac{1 + \sum_{k=1}^{n} a_{p,k}^M \tau^k}{1 + \sum_{k=1}^{n+2} b_{p,k}^M \tau^k} \tag{8}$$

with $n = 1$, yielding four parameters for G_{Mp} and the two TPE parameters α and β. In their second fit (ABGG Fit 2), the cross section and polarization transfer data were fit simultaneously, using 4 parameter fits to G_{Ep} and G_{Mp} along with the two TPE parameters.

Qattan and Alsaad [21] proposed a different empirical parametrization for the function $F(Q^2, \varepsilon)$. The function $F(Q^2, \varepsilon)$ was double Taylor series expanded as a polynomial of order n keeping only terms linear in ε but without constraining the TPE amplitudes by enforcing the Regge limit. In their final result, labeled fit III, the reduced cross section σ_R was parametrized as:

$$\sigma_R = G_{Mp}^2\Big(1 + \frac{\varepsilon}{\tau}R^2\Big) + \varepsilon f(Q^2), \tag{9}$$

where for the extraction from a fixed-Q^2 data set, $f(Q^2)$ is just a constant. Throughout this text, Eq. (9) will be referred to as the QA parametrization.

As noted in some previous extractions [19, 20, 22, 29], small angle comparisons of positron to electron scattering set tight limits on the TPE effects and TPE calculations [9, 18, 24, 25] show that the contribution should be zero at $\varepsilon = 1$. Therefore, we perform an updated version of the fit from Ref. [21] using a parametrization which maintains the linear correction in ε but yields $F(Q^2, \varepsilon) = 0$ at $\varepsilon = 1$. Based on the parametrization from Borisyuk and Kobushkin [22], we take the following:

$$\sigma_R = G_{Mp}^2\Big(1 + \frac{\varepsilon}{\tau}R^2\Big) + 2a(1-\varepsilon)G_{Mp}^2, \tag{10}$$

for our updated extraction. Throughout this text, Eq. (10) will be referred to as the BK parametrization. Because the recoil polarization ratio G_{Ep}/G_{Mp} was experimentally confirmed to be independent of ε [26], the ratio $R = G_{Ep}/G_{Mp}$ was fixed to be that of the recoil polarization ratio or Eq. (3), as in the analysis of Ref. [21]

III. RESULTS AND DISCUSSION

In this article we do the following:

(1) We extend the analysis of Ref. [21], extracting the TPE contributions to σ_R using both the QA and BK parametrizations for the TPE amplitude. We also include additional data sets [34–36], that were not included in the original analysis. For the data from Qattan, *et al.* [41], we use the published results, including the ε-dependent systematic uncertainties, yielding somewhat modified results than in the previous analysis [21].

(2) We take the proton form factors and TPE amplitudes extracted using the QA and BK parametrizations and compare them to those obtained using the extracted TPE corrections Refs. [19, 30, 37] and the TPE calculation of Ref. [38]. We also use our results and the previous parametrizations to determine the ratio $R^{e^+e^-}$. We use these results to examine the Q^2 dependence of the extracted TPE corrections, the consistency of the different extractions, and discuss the impact of the different assumptions used in these analyses.

(3) We compare the TPE contributions as extracted using these different approaches to more recent extractions [20, 22] which attempt to extract the TPE amplitudes using additional constraints that come from a recent measurement of the ε dependence of G_{Ep}/G_{Mp} at $Q^2 = 2.50$ $(\mathrm{GeV/c})^2$ [26].

A. Form Factors and the TPE Amplitudes

We begin with the extraction of the form factors and TPE contributions based on the QA parametrization, Eq. (9). The results of this fit for the data sets of Refs. [32, 34–36, 39–41] are given in Table I. The extraction follows the procedure of fit III from Ref. [21], with the fit to the polarization transfer data, Eq. (3), used to constrain R, leaving G_{Mp} and f as the two fit parameters. We also extract the TPE contributions using the BK parametrization Eq. (10). Table II lists the results of the fit.

Note that for these older data sets, we use the same cross sections used in the analysis of Ref. [30, 42], where missing higher older radiative corrections terms such as the Schwinger term and additional vacuum polarization contributions from muon and quark loops have been applied. See Ref. [43] for tabulated electron-proton elastic scattering cross sections data.

Figure 1 shows the values of $(G_{Ep}/G_D)^2$ and $(G_{Mp}/\mu_p G_D)^2$ obtained using the QA and BK parametrizations (shown as hollow and solid circles, respectively). The solid curves are fits to the extracted form factors from previous phenomenological analyses: Ref. [31] (ABGG Fit I and ABGG Fit II), and Ref. [19] (Arrington $Y_{2\gamma}$ Fit), and the form factors extracted based on a calculation of the TPE contributions from Ref. [38] (AMT Fit). The dotted line is the global Rosenbluth extraction from Ref. [30] (Arrington σ_R Fit), which does not include TPE corrections.

The QA results for G_{Mp} are typically 2–10% lower, with the larger corrections generally associated with

TABLE I: The form factors and TPE parameters obtained using the QA parametrization, Eq. (9), as a function of Q^2 (given in units of $(\mathrm{GeV/c})^2$). The TPE correction is extracted based on the assumption that it fully resolves the difference between $\mu_p G_{Ep}/G_{Mp}$ as extracted from the given Rosenbluth extraction and the value from the polarization transfer parametrization of Eq. (3). The overall normalization uncertainty for each data set (typically 1.5–3%) is not taken into account in this extraction. See text for complete details.

Q^2 (GeV/c)^2	$(G_{Mp}/\mu_p G_D)^2$	$(G_{Ep}/G_D)^2$	$f(Q^2)\times 100$	χ^2_ν
Andivahis [32] (taken from Ref. [21])				
1.75	1.106±0.014	0.669±0.009	0.32±0.14	0.30
2.50	1.111±0.013	0.514±0.006	0.07±0.04	0.53
3.25	1.092±0.018	0.371±0.006	0.05±0.02	0.16
4.00	1.068±0.017	0.251±0.004	0.02±0.01	0.51
5.00	1.029±0.017	0.130±0.002	0.01±0.005	0.93
Walker [39] (taken from Ref. [21])				
1.00	1.024±0.055	0.785±0.042	2.40±1.97	0.72
2.00	1.020±0.037	0.563±0.020	0.67±0.18	0.65
2.50	1.040±0.034	0.483±0.016	0.28±0.08	0.98
3.00	1.010±0.045	0.378±0.017	0.18±0.06	0.19
Christy [40] (taken from Ref. [21])				
0.65	0.916±0.061	0.777±0.052	13.07±6.33	0.02
0.90	1.047±0.036	0.826±0.028	1.58±1.81	1.37
2.20	1.110±0.030	0.574±0.016	0.13±0.12	1.07
2.75	1.115±0.021	0.468±0.009	0.07±0.05	0.04
3.75	1.087±0.030	0.291±0.008	0.03±0.02	1.15
4.25	1.023±0.024	0.210±0.005	0.05±0.01	0.55
5.25	1.015±0.065	0.106±0.007	0.02±0.01	0.78
Qattan [41]				
2.64	1.108±0.007	0.486±0.003	6.39±1.10	0.35
3.20	1.098±0.008	0.381±0.003	8.13±1.32	0.54
4.10	1.064±0.010	0.237±0.002	10.80±1.78	0.14
Bartel [34]				
1.169	1.045±0.029	0.761±0.021	1.63±0.89	0.26
1.75	1.103±0.029	0.667±0.018	−0.03±0.30	0.01
Litt [35]				
1.50	0.970±0.247	0.637±0.162	1.86±2.67	0.01
2.00	0.961±0.230	0.534±0.128	0.86±1.09	1.10
2.50	1.031±0.062	0.477±0.029	0.23±0.15	0.65
3.75	0.960±0.081	0.257±0.022	0.10±0.05	0.32
Berger [36]				
0.389	0.970±0.037	0.884±0.034	−0.9±12.8	0.48
0.584	0.970±0.017	0.837±0.015	5.27±2.78	0.38
0.779	1.008±0.025	0.823±0.020	1.82±2.22	0.55
0.973	1.005±0.032	0.776±0.025	3.37±1.65	0.81
1.168	1.047±0.048	0.763±0.035	2.35±1.94	0.29
1.363	1.076±0.046	0.738±0.031	0.29±1.22	0.58
1.558	1.063±0.057	0.685±0.036	1.71±1.48	1.12
1.752	1.129±0.077	0.682±0.047	0.07±1.21	0.75

TABLE II: The form factors and TPE parameters obtained using the BK parametrization, Eq. (10), as a function of Q^2 (given in units of $(\mathrm{GeV/c})^2$). The TPE correction is extracted based on the assumption that it fully resolves the difference between $\mu_p G_{Ep}/G_{Mp}$ as extracted from the given Rosenbluth extraction and the value from the polarization transfer parametrization of Eq. (3). The overall normalization uncertainty for each data set (typically 1.5–3%) is not taken into account in this extraction. See text for complete details.

Q^2	$(G_{Mp}/\mu_p G_D)^2$	$(G_{Ep}/G_D)^2$	$a(Q^2)\times 100$	χ^2_ν	N_p
Andivahis [32]					
1.75	1.158±0.012	0.700±0.007	−2.25±0.94	0.30	4
2.50	1.147±0.010	0.531±0.004	−1.57±0.88	0.53	7
3.25	1.149±0.013	0.390±0.004	−2.48±1.16	0.16	5
4.00	1.128±0.012	0.265±0.003	−2.64±1.10	0.51	6
5.00	1.090±0.014	0.138±0.002	−2.82±1.24	0.93	5
Walker [39]					
1.00	1.101±0.012	0.844±0.009	−3.50±3.29	0.57	3
2.00	1.183±0.009	0.656±0.005	−6.92±1.82	0.56	8
2.50	1.177±0.010	0.545±0.005	−5.84±1.90	0.74	6
3.00	1.178±0.014	0.445±0.005	−7.15±2.30	0.18	5
Christy [40]					
0.65	1.058±0.010	0.897±0.009	−6.71±3.18	0.01	3
0.90	1.086±0.011	0.856±0.009	−1.77±2.10	1.37	3
2.20	1.154±0.014	0.597±0.007	−1.92±1.84	1.07	3
2.75	1.162±0.014	0.487±0.006	−2.04±1.34	0.04	3
3.75	1.147±0.020	0.307±0.005	−2.61±2.03	1.47	3
4.25	1.169±0.021	0.240±0.004	−6.22±1.64	0.55	3
5.25	1.123±0.041	0.117±0.004	−4.83±4.50	0.78	3
Qattan [41]					
2.64	1.174±0.006	0.515±0.003	−2.81±0.49	0.35	5
3.20	1.183±0.007	0.411±0.003	−3.60±0.57	0.54	4
4.10	1.176±0.011	0.262±0.002	−4.77±0.78	0.14	3
Bartel [34]					
1.169	1.125±0.022	0.819±0.016	−3.57±1.89	0.26	3
1.75	1.099±0.028	0.665±0.017	+0.18±2.21	0.01	3
Litt [35]					
1.50	1.157±0.022	0.759±0.015	−8.09±10.2	0.01	3
2.00	1.169±0.023	0.649±0.013	−8.86±6.80	1.10	4
2.50	1.143±0.011	0.529±0.005	−4.90±2.81	0.65	9
3.75	1.154±0.016	0.309±0.004	−8.40±3.59	0.32	3
Berger [36]					
0.389	0.966±0.011	0.881±0.010	+0.17±2.35	0.48	7
0.584	1.014±0.009	0.876±0.008	−2.20±1.14	0.38	14
0.779	1.038±0.018	0.848±0.014	−1.48±1.80	0.55	6
0.973	1.106±0.022	0.854±0.017	−4.55±2.16	0.81	5
1.168	1.162±0.055	0.846±0.040	−4.95±4.04	0.29	4
1.363	1.099±0.054	0.753±0.037	−1.01±4.20	0.58	4
1.558	1.265±0.126	0.815±0.081	−8.01±6.26	1.12	3
1.752	1.141±0.135	0.690±0.082	−0.54±9.20	0.75	3

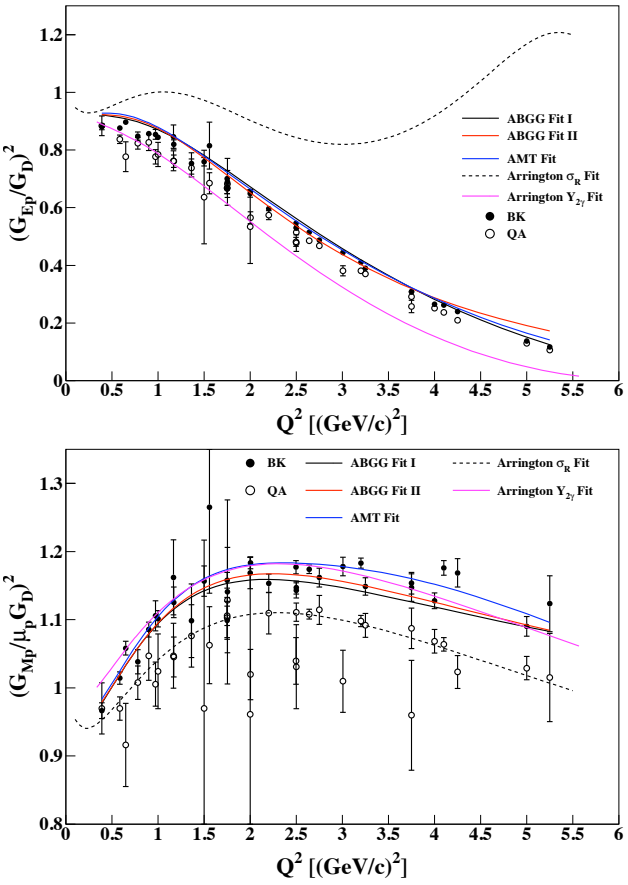

FIG. 1: (Color online) $(G_{Ep}/G_D)^2$ [top] and $(G_{Mp}/\mu_p G_D)^2$ [bottom] as obtained from Refs. [32, 34–36, 39–41] using the QA and BK parametrizations. Also shown are the ABGG I and ABGG II fits [31], the AMT fit [38], the Arrington $Y_{2\gamma}$ Fit [19], and the Arrington σ_R Fit [30] which does not include any TPE contributions or polarization data.

points that are very poorly constrained in the QA fit due to their lack of low-ε data. This simply reflects the fact that the QA parametrization yields no TPE contribution at $\varepsilon = 0$, and thus the (linear) extrapolation to the *anchor point* at $\varepsilon = 0$ is unchanged by the application of the extracted TPE contributions, while the extrapolation is modified by the TPE contributions for the BK parametrization. Note that because they use the same PT parametrization for $\mu_p G_{Ep}/G_{Mp}$, the G_{Ep} values are also lower by the same amount for the QA extraction. In addition, the uncertainties are much larger in the QA extraction for some kinematics. Most experiments tend to have a large part of their data at large ε values, so there is a significant extrapolation to $\varepsilon = 0$ in the QA extraction, yielding a larger uncertainty in the overall normalization. For the BK parametrization, the normalization is fixed at the $\varepsilon = 1$ value. This reduction in the uncertainties demonstrates one of the important strengths of the polarization transfer measurements, as they significantly reduce the uncertainty associated with the extraction to $\varepsilon = 0$. While the uncertainty on the PT data is small, neglecting this uncertainty in the fit (as we and some other extractions do), yields a small underestimate underestimate of the uncertainty. The uncertainties associated with this, and other assumptions that go into the phenomenological extractions, will be discussed in Sec. III B.

In the extraction of $(G_{Ep}/G_D)^2$, there is a large difference between the TPE-uncorrected result (Arrington σ_R) and the extractions that apply corrections for TPE contributions, because the LT extraction of G_{Ep} at large Q^2 is extreme sensitivity to any angular-dependent TPE corrections. Nearly all of the other fits extractions are in excellent agreement, but this is simply because they all explain the difference between the LT and PT extractions of G_{Ep}/G_{Mp} in terms of a nearly-linear correction to the reduced cross section. Therefore, these analyses will, by construction, ensure that the final result for G_{Ep}/G_{Mp} will be consistent with the polarization data, thus yielding nearly identical values for G_{Ep} except for small differences in the extracted values of $(G_{Mp}/\mu_p G_D)^2$, most clearly seen in the QA extraction. The quality of the agreement shows that the small non-linearities in the ABGG analysis and the choice of cross section data sets and parametrization for the polarization transfer measurements has little impact. The AMT analysis applies TPE contributions based on a hadronic calculation [10], with a small additional contribution designed to more fully resolve the discrepancy for $Q^2 > 2$ (GeV/c)^2, where the calculated TPE do not bring the LT and PT results into perfect agreement. Because of this additional contribution, and the neglect of TPE contributions to the polarization data, this analysis must also yield results consistent with the other analyses at large Q^2. The only analysis that yields different results is the Arrington Y_{2g} fit, where the extraction of all three amplitudes allows for a calculation of the TPE contribution to the polarization transfer data, yielding a noticeable downward shift in the value of $\mu_p G_{Ep}/G_{Mp}$ and thus $(G_{Ep}/G_D)^2$. However, the size and even the sign of this correction depend on the assumptions made in trying to separate the three TPE amplitudes. Thus, the deviation from the other fits is at best an indication of the possible uncertainty in these extractions. This will be addressed further when we compare to other extractions that include TPE contributions to the polarization data in Sec. III B.

For the extraction of $(G_{Mp}/\mu_p G_D)^2$, the BK results are in good agreement with previous extractions that include TPE, while the QA results are more consistent with the Arrington σ_R fit which neglects TPE. The BK and ABGG other extractions assume no TPE contribution and an approximately linear correction to the reduced cross section, as discussed above. Because they require very similar corrections to the ε dependence of σ_R to resolve the discrepancy in $\mu_p G_{Ep}/G_{Mp}$ measurements, they have very similar corrections to $(G_{Mp}/\mu_p G_D)^2$, which simply relates to the low-ε value of the correction. The Arrington Y_{2g} fit is the only extraction in which the polarization transfer results for G_{Ep}/G_{Mp} are modified

by TPE contributions, but while the overall size of the TPE correction required to resolve the LT-PT discrepancy is somewhat larger in this case, the absolute correction to the cross section is small, yielding very similar values for $(G_{Mp}/\mu_p G_D)^2$.

Figure 2 shows the fit parameter $a(Q^2)$ as a function of Q^2 for all data sets. The parameter $a(Q^2)$ is on the few percent level, and for the most part, increases in magnitude with increasing Q^2. Note that the TPE contribution to the cross section is $F(Q^2,\varepsilon) = 2a(1-\varepsilon)G_{Mp}^2$, and thus at high Q^2, the slope introduced by the TPE correction is $2a$. The extracted TPE contributions from the different data sets is relatively consistent, and shows a slow increase in the TPE contribution as Q^2 increases.

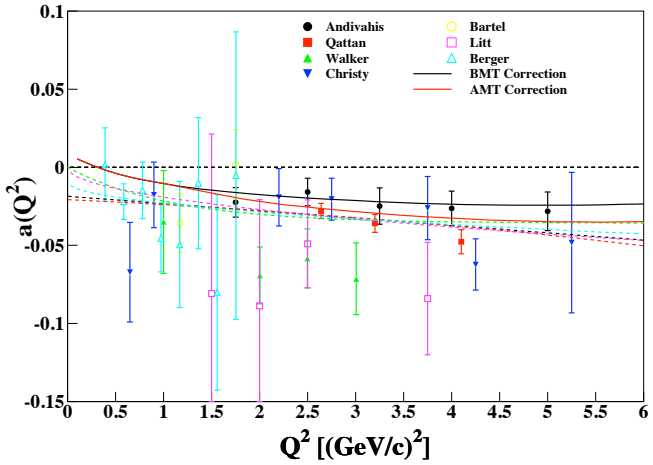

FIG. 2: (Color online) The fit parameter $a(Q^2)$ as obtained using the BK parametrization from the data of Refs. [32, 34–36, 39–41]. The dashed curves correspond to fits to the Q^2 dependence using different parametrizations (see text) and the solid lines correspond to the values of $a(Q^2)$ determined by fitting to the TPE calculations of Ref. [10], and the TPE correction of Ref. [38] which adds and additional phenomenological TPE contribution at higher Q^2.

In an attempt to parametrize the Q^2 dependence of the parameter $a(Q^2)$, several different functional forms were tried and are plotted as dashed lines in Fig. 2. These fits all give reasonable reduced χ^2 values, $1.04 < \chi^2_\nu < 1.10$. The lowest χ^2_ν value was obtained using the form $a(Q^2) = \alpha\sqrt{Q^2}$ with α=−0.0191±0.0014 (magenta dashed line in Fig. 2). The full spread of the fits is below 0.005 for $1<Q^2<4$ (GeV/c)^2, although at lower Q^2 values, none of the extractions are precise and the behavior is largely unconstrained below $Q^2 \approx 1.5$ (GeV/c)^2. For our global fit, we take

$$a(Q^2) = -0.0191\sqrt{Q^2} \pm 0.0014\sqrt{Q^2} \pm 0.003 \qquad (11)$$

where the first uncertainty is the fit uncertainty in α, and the second is the systematic error band included to account for the model dependence of the fit for $1.5 < Q^2 < 4$ (GeV/c)^2.

Figure 2 also shows curves for $a(Q^2)$ based on the hadronic TPE correction of Ref. [10], along with the version used in Ref. [38] which includes a small additional contribution at high Q^2 values. The version used in the global analysis of the form factors [38] is in good agreement with our fit for $Q^2 \gtrsim 2$ (GeV/c)^2, where the data provides significant constraints on the TPE contributions. Note that the calculated TPE corrections, as well as those of Refs. [44, 45], show a change of sign in the TPE effects for $Q^2 < 0.5$ (GeV/c)^2. This is not seen in the data, although the constraints at low Q^2 are insufficient to make strong conclusions in this region.

The fact that the low Q^2 behavior is inconsistent with the calculations is not entirely surprising. Our extraction, like most similar phenomenological analyses, assumes that TPE contributions can be significant for the cross section measurements, but negligible for polarization data. However, both the hadronic [10] and partonic [46] calculations suggest that the TPE contributions are at the few percent level for both observables. The main difference is that the impact of the correction on the extracted form factors is amplified for G_{Ep} at high Q^2, where the form factor is extracted from a small angular dependence in the cross section which can be noticeably modified by a few percent TPE contribution. At low Q^2, the TPE contribution is not amplified in the extraction of the form factors from the cross section data, so neglecting the contributions to the polarization transfer data will not be reliable. In addition, because the difference between $\mu_p G_{Ep}/G_{Mp}$ from Rosenbluth and polarization transfer measurements becomes small at low Q^2, neglecting the uncertainty in the polarization transfer extraction of $\mu_p G_{Ep}/G_{Mp}$ leads to a significant underestimate of the uncertainties below 1 (GeV/c)^2.

In Fig. 3, we compare the ε dependence of the TPE corrections based on the different extractions based on the data from Ref. [32]. In addition to the extractions from the QA and BK parametrizations, we show the ABGG Fit I (black line), ABGG Fit II (red line), the Arrington $Y_{2\gamma}$ Fit (blue line). Most of the extractions yield similar slopes, with the QA extraction differing from the others in that the TPE contribution goes to zero at $\varepsilon = 0$. The Arrington $Y_{2\gamma}$ parametrization has a somewhat larger slope, because of the inclusion of TPE contributions which reduce R as measured in polarization experiments, thus necessitating a greater decrease to R as extracted in a Rosenbluth separation. The TPE corrections increase slowly with Q^2 except for the ABGG fits which show essentially no Q^2 dependence. In these extractions, the Q^2 dependence of the TPE contribution is taken to go as $G_D^2(Q^2)$, and thus they are a nearly constant fractional correction to the cross section at large Q^2 values, where $G_M \approx \mu_p G_D$ dominates the cross section.

B. The $R^{e^+e^-}$ Ratio

The function $F(Q^2,\varepsilon)$ which represents the interference of the OPE and TPE amplitudes changes sign depending on the charge of the projectile, yielding an ampli-

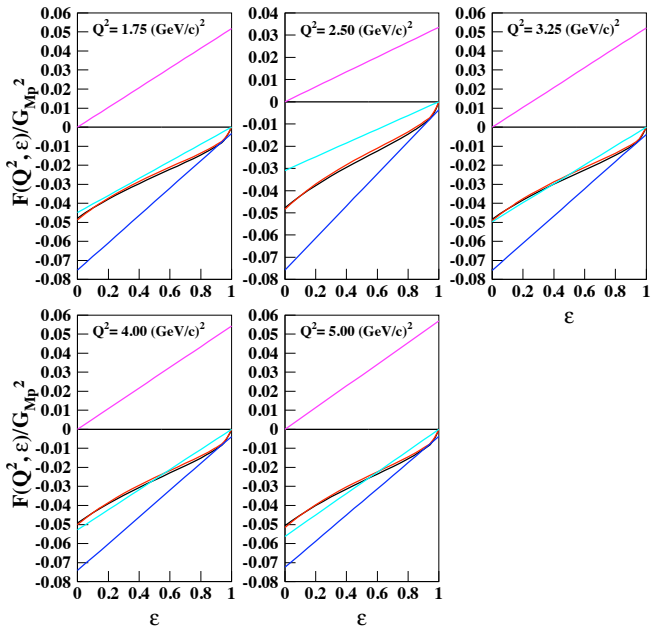

FIG. 3: (Color online) The Ratio $F(Q^2,\varepsilon)/G_{Mp}^2$ as a function of ε at Q^2 = 1.75, 2.50, 3.25, 4.0, and 5.0 (GeV/c)^2 from Ref. [32] determined using the QA parametrization (magenta line), the BK parametrization (cyan line), the ABGG Fit I (black line) and the ABGG Fit II (red line), and the Arrington $Y_{2\gamma}$ Fit (blue line).

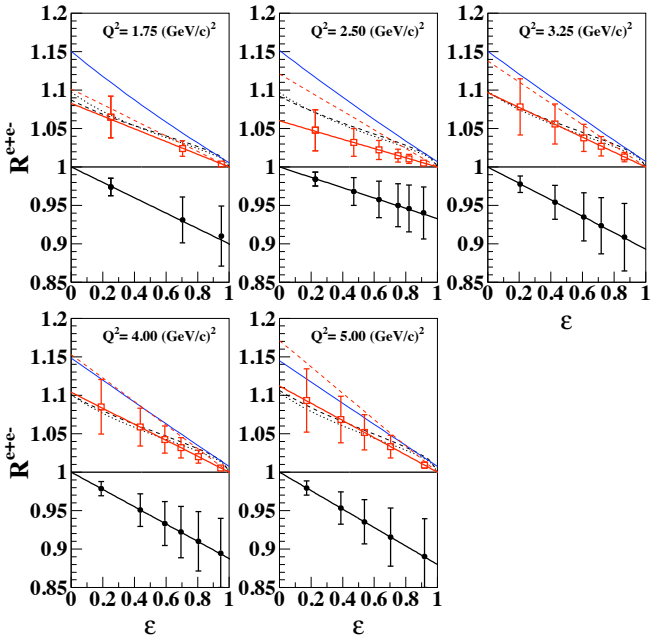

FIG. 4: (Color online) $R^{e^+e^-}$ as a function of ε at Q^2 = 1.75, 2.50, 3.25, 4.0, and 5.0 (GeV/c)^2 from Ref. [32] determined using the QA parametrization (solid black circles), and the BK parametrization (open red squares). The solid black and red lines through the data are calculated using Eqs. (12) and (13), respectively, while the dashed red line is the global fit from the BK extraction Eq. (11). Also shown are results of the Arrington $Y_{2\gamma}$ Fit (solid blue line), the ABGG Fit I (black dashed line) and the ABGG Fit II (black dotted line).

fied signal when taking the ratio of electron and positron scattering. The ratio $R^{e^+e^-}(Q^2,\varepsilon)$, defined by Eq. (5), is determined simply by changing the sign in front of the TPE amplitudes. We determined the ratio $R^{e^+e^-}$ using the form factors and the TPE amplitude extracted using the QA and BK parametrizations. These ratios will then be compared to those obtained from other analyses [10, 19, 20, 22, 37], and used to make predictions for new and recently completed measurements [47–51].

Figure 4 shows the ratio $R^{e^+e^-}$ as a function of ε extracted from the data of Ref. [32] using the QA parametrization (solid black circle) and the BK parametrization (open red squares), along with the previous extractions. The ratio $R^{e^+e^-}$ as determined using the QA parametrization is always equal to or less than unity, while the other parametrizations force $R^{e^+e^-} = 0$ at $\varepsilon = 1$, yielding a ratio that is always equal to or larger than one. Because measurements of $R^{e^+e^-}$ put significant constraints on deviations from unity at $\varepsilon = 1$, we exclude the QA parametrization from further comparisons. As seen in Figs. 3 and 4, the ε dependence is very similar to that of the BK fit, except for the overall offset.

For a better comparison between the two parametrizations, we fit the ratio extracted using the QA parametrization to the form

$$R^{e^+e^-}(Q^2,\varepsilon) = 1 + B(Q^2)\varepsilon, \qquad (12)$$

and that extracted using the BK parametrization to

$$R^{e^+e^-}(Q^2,\varepsilon) = 1 - B(Q^2)(1-\varepsilon), \qquad (13)$$

with $B(Q^2)$ being the parameter of the fit and represents the slope. The values of $B(Q^2)$ from the BK fit are given in Table III and shown as a function of Q^2 for each experiment in Fig. 5. The slope $B(Q^2)$ is negative and grows in magnitude with increasing Q^2 value almost for most data sets. We also compare the results to a reference curve corresponding to our global fit Eq. (11).

In Figs. 4 and 6, we compare previous TPE extractions to our results for the kinematics of the two highest precision data sets [32, 41]. The ratio $R^{e^+e^-}$ as predicted by ABGG Fit 1 and ABGG Fit 2 are nearly identical, but smaller than the Arrington $Y_{2\gamma}$ Fit. For the Andivahis data, our extraction is in generally good agreement with the ABGG fits, but the Qattan data yield larger TPE corrections, especially at their higher Q^2 values.

At present, precise measurements of $R^{e^+e^-}$ are limited to relatively low Q^2 or large ε, making it difficult to directly compare the data to estimates of the ε dependence of TPE at high Q^2 extracted from comparisons of the Rosenbluth and polarization measurements. As stated in Ref. [29], if TPE corrections are responsible for the discrepancy between the Rosenbluth and recoil-polarization data, a 5–8%, linear or quasi-linear, ε-dependent correc-

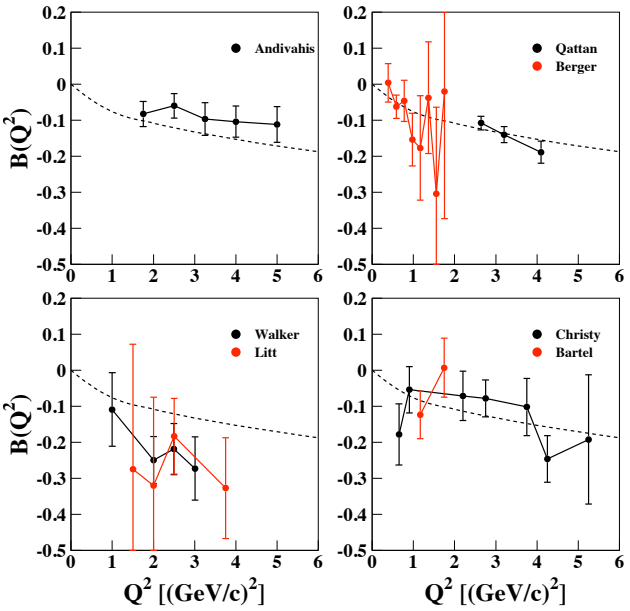

FIG. 5: (Color online) The slope $B(Q^2)$ as a function of Q^2 as determined using the BK parametrization. The solid lines connecting the data points are to guide the eye, while the black dashed curve is our global best fit.

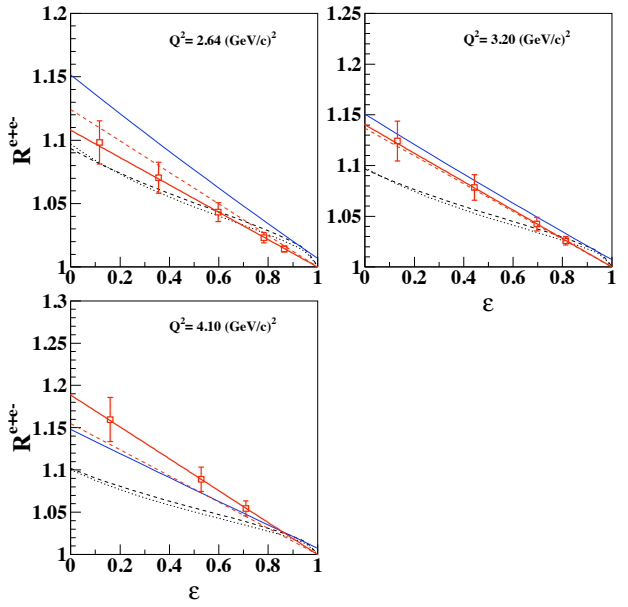

FIG. 6: (Color online) $R^{e^+e^-}$ as a function of ε as extracted from Ref. [41] using the BK parametrization (square points and solid red line). The red dashed lines show the global fit of Eq. (11). Also shown are the results of the Arrington $Y_{2\gamma}$ Fit (solid blue line), the ABGG Fit I (black dashed line) and the ABGG Fit II (black dotted line).

TABLE III: The values of the slope $B(Q^2)$ as obtained using the QA and BK parametrizations by fitting to Eqs. (12) and (13), respectively.

Q^2(GeV/c)^2	$B(Q^2)$ [QA]	$B(Q^2)$ [BK]
		Andivahis *et al.* (Ref. [32])
1.75	−0.0999±0.0434	−0.0827±0.0346
2.50	−0.0672±0.0378	−0.0600±0.0337
3.25	−0.1067±0.0513	−0.0967±0.0451
4.00	−0.1124±0.0483	−0.1037±0.0434
5.00	−0.1200±0.0537	−0.1119±0.0494
		Walker *et al.* (Ref. [39])
1.00	−0.1571±0.1291	−0.1090±0.1022
2.00	−0.3268±0.0874	−0.2499±0.0656
2.50	−0.2681±0.0811	−0.2186±0.0710
3.00	−0.3378±0.1142	−0.2729±0.0878
		Christy *et al.* (Ref. [40])
0.65	−0.3274±0.1588	−0.1784±0.0846
0.90	−0.0786±0.0904	−0.0542±0.0645
2.20	−0.0813±0.0744	−0.0713±0.0684
2.75	−0.0871±0.0581	−0.0781±0.0513
3.75	−0.1116±0.0880	−0.1022±0.0796
4.25	−0.2872±0.0791	−0.2461±0.0648
5.25	−0.2141±0.2037	−0.1921±0.1790
		Qattan *et al.* (Ref. [41])
2.64	−0.1228±0.0212	−0.1078±0.0187
3.20	−0.1585±0.0258	−0.1401±0.0223
4.10	−0.2135±0.0352	−0.1886±0.0307
		Bartel *et al.* (Ref. [34])
1.169	−0.1707±0.0933	−0.1239±0.0658
1.750	+0.0079±0.0935	+0.0068±0.0820
		Litt *et al.* (Ref. [35])
1.50	−0.3909±0.5630	−0.2748±0.3471
2.00	−0.4382±0.5581	−0.3202±0.2457
2.50	−0.2200±0.1404	−0.1830±0.1050
3.75	−0.4059±0.1935	−0.3271±0.1400
		Berger *et al.* (Ref. [36])
0.389	+0.0079±0.1108	+0.0039±0.0534
0.584	−0.1087±0.0579	−0.0623±0.0324
0.779	−0.0705±0.0864	−0.0464±0.0572
0.973	−0.2291±0.1121	−0.1534±0.0731
1.168	−0.2516±0.2075	−0.1769±0.1447
1.363	−0.0462±0.1942	−0.0374±0.1545
1.558	−0.4284±0.3530	−0.3037±0.2395
1.752	−0.0232±0.3807	−0.0205±0.3527

tion to the electron cross section is required to resolve the discrepancy at high Q^2. This implies that $R^{e^+e^-}$ at high Q^2 should have a 10–16% quasi-linear ε dependence, with $R^{e^+e^-}$ decreasing as ε increases. The existing $R^{e^+e^-}$ data provide some evidence for such a ε dependence, but the significance is only 3σ and limited to low Q^2 data, where the ε-dependence is observed to be (5.7±1.8)% [29]. This corresponds to $B(Q^2) = 0.057$, but the extraction uses all data below $Q^2 = 2$ (GeV/c)^2, corresponding to an av-

erage Q^2 values of approximately 0.5 (GeV/c)^2, making the result consistent with the low Q^2 extractions presented here. Relatively precise data do exist at large ε and moderate Q^2 values, suggesting that $R^{e^+e^-} \approx 1$ for $\varepsilon \to 1$, as assumed in most of the extractions presented here.

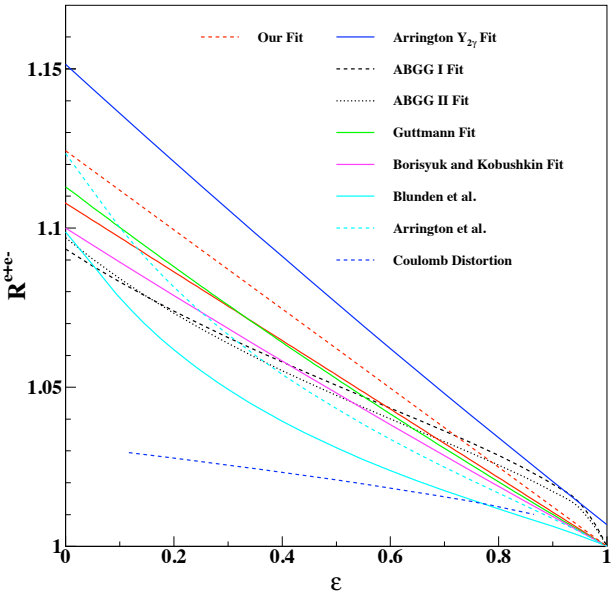

FIG. 7: (Color online) Ratio $R^{e^+e^-}$ as a function of ε at $Q^2 = 2.64$ (GeV/c)^2. In addition to the curves shown in Fig. 6, we also show the corrections from Blunden *et al.* [10], and the extractions from Guttmann *et al.* [20] and Borisyuk and Kobushkin [22]. Note that the extraction of Ref. [22] was performed at $Q^2 = 2.50$ (GeV/c)^2. The uncertainties in our fit Eq. (11) correspond to an uncertainty of ± 0.15 at ε=0.

Finally, we make an additional comparison of the ε dependence at $Q^2 = 2.64$ (GeV/c)^2, including two recent extractions which take advantage of new measurements of the ε dependence of the recoil polarization data [26]. These are similar to the earlier attempts to separate the individual TPE amplitudes [15, 19], but because of the new data on the ε dependence of the polarization measurement of $\mu_p G_{Ep}/G_{Mp}$ and the polarization component P_l, fewer assumptions have to be made as to the contribution of the different amplitudes.

Guttmann *et al.* [20], used the measurements of the ε dependence of P_l and P_t/P_l [26] along with the ε dependence of the cross section [41] to constrain the three TPE amplitudes Y_M, Y_E, and Y_3. By writing the observables in terms of Born values and the TPE amplitudes and keeping only the larger TPE correction (i.e. neglecting those that are suppressed by kinematic or other factors), they observe that the corrections to P_l/P_l^{Born} are largely determined by Y_3 and the corrections to P_t/P_l (which shows no ε-dependence) come from a sum of Y_3 and Y_E. Thus, the ε dependence of P_l is used to determine Y_3, after choosing an ε dependence based on constraints from a pQCD calculation [52], and the lack of TPE contribution to P_t/P_l then constrains Y_E. This allows Y_M to be extracted based on the difference between the predicted and measured values of the reduced cross section as a function of ε. This accounts for all of the uncertainty in the extraction of the PT result for $\mu_p G_{Ep}/G_{Mp}$ based on the assumption that there is no ε-dependent TPE correction, but does not account for the fact that the data are still consistent with a ε dependence of a few percent over the full ε range. Their extracted amplitudes are used to determine $R^{e^+e^-}$ at $Q^2 = 2.64$ (GeV/c)^2, which reaches a maximum value of 1.11 ± 0.16, is compared to the other extractions in Fig. 7.

The analysis of Borisyuk and Kobushkin [22] takes a similar approach, although they use a different linear combination of amplitudes than Ref. [15]. Again, the ε dependence of P_t/P_l is taken to be zero [26], and the correction to the cross section is taken to be linear [17]. Data from available electron-proton scattering cross sections in the range of $2.20 \le Q^2 \le 2.80$ (GeV/c)^2 were interpolated to $Q^2 = 2.5$ (GeV/c)^2 to extract the amplitudes at a fixed Q^2 value. This yields an extraction in terms of a single amplitude, and using the parametrization of Eq. (10), they obtain a value of $a = -0.0250 \pm 0.0035$, corresponding to a peak $R^{e^+e^-}$ value of 1.11 ± 0.16.

Note that the values and uncertainties in our extraction and both of these extractions of the TPE amplitudes are very similar. While the details of the assumptions made in extracting the TPE amplitudes affect the prediction they make for polarization observables, they both assume that there is no TPE contribution to the polarization transfer ratio, and thus are extracting amplitudes designed to induce a linear correction to the reduced cross section to make it consistent with the PT data. So for the observables related to the form factor extraction, this is the same assumption made in all of the phenomenological extractions except for the Arrington $Y_{2\gamma}$ fit. Similarly, these extractions typically neglect some of the uncertainties associated with the TPE contributions to the PT measurements. All of them ignore the uncertainty in the extracted value of $\mu_p G_{Ep}/G_{Mp}$ or the impact of a possible ε dependence, and most of the phenomenological extractions ignore both. The Arrington $Y_{2\gamma}$ fit includes the uncertainty in the extraction of $\mu_p G_{Ep}/G_{Mp}$ from PT data, but not the uncertainty associated with the TPE. One can take the difference between the Arrington $Y_{2\gamma}$ fit and the other extractions of G_{Ep}, Fig. (1), as an estimate of the latter uncertainty, but the TPE impact on the PT data in this analysis is rather large, so this difference is probably better treated as an upper limit in the uncertainty, at least for Q^2 up to 3–4 (GeV/c)^2. A shift in the PT values of $\mu_p G_{Ep}/G_{Mp}$ of 0.02 at $Q^2 \approx 1$ (GeV/c)^2 and 0.05 for $Q^2 \approx 5$ (GeV/c)^2 would yield a modified TPE correction, changing the extracted value of $a(Q^2)$ by 0.003–0.005 (and the low ε value of $R^{e^+e^-}$ in Fig. 7 by 0.01–0.02, which is comparable to the total uncertainty we quote in the fit Eq. (11). This shift in $\mu_p G_{Ep}/G_{Mp}$ is at the level of the uncertainties in the polarization extraction. It is also comparable to the level at which the ε dependence of the TPE contributions to the polarization

data are constrained. Thus, the uncertainty neglected when the uncertainties and/or TPE contributions to the PT data are neglected are comparable to the total uncertainties obtained in these extractions.

There has been a recent push to make new measurements of the ratio $R^{e^+e^-}$, focusing on small ε, where TPE contributions appear to be largest. The first is the VEPP-3 experiment [47–49], where the internal target at the VEPP-3 electron-positron storage ring at Novosibirsk was used to extract the ratio $R^{e^+e^-}$ at $Q^2 = 1.60$ (GeV/c)^2 and $\varepsilon \approx 0.4$. A raw $R^{e^+e^-}$ ratio of 1.056±0.011 was obtained, which must be reduced by the charge-dependent bremsstrahlung correction, estimated to be ∼3%. The Blunden, *et al.*, calculation [10] predicts $R^{e^+e^-} = 1.036$ (1.043 with the additional contribution included in Ref. [38]). Our global fit predicts $R^{e^+e^-} = 1.061 \pm 0.009$, but the Q^2 value is low enough that the extraction is not expected to be very reliable.

The second experiment is Jefferson Lab experiment E07-005 [50], where a mixed beam of e^+ and e^- produced via pair production from a secondary photon beam, was used to simultaneously measure $\sigma(e^+p \to e^+p)$ and $\sigma(e^-p \to e^-p)$ elastic scattering cross sections. Cross sections in the kinematical range of $0.5 < Q^2 < 2.0$ (GeV/c)^2 and $0.2 < \varepsilon < 0.9$ can be measured. The third is the OLYMPUS experiment [51], where the DORIS lepton storage ring at DESY will be used to extract the ratio $R^{e^+e^-}$ from $Q^2 = 0.6$ (GeV/c)^2 and $\varepsilon = 0.90$, to $Q^2 = 2.2$ (GeV/c)^2 and $\varepsilon = 0.35$.

IV. CONCLUSIONS

In conclusion, we extracted the elastic electromagnetic form factors of the proton using two different parametrizations for the OPE-TPE interference function $F(Q^2, \varepsilon)$, the QA parametrization Eq. (9) and the BK parametrization Eq. (10). Both parametrizations are linear in ε, but make different assumptions as to where the TPE contributions vanish. In the BK parametrization, the TPE correction to σ_R was constrained by enforcing the Regge limit which was not done in the QA parametrization. In both parametrizations, we constrained $\mu_p G_{Ep}/G_{Mp}$ using recoil polarization data. The values of G_{Mp} and G_{Ep} extracted using the QA parametrization are smaller than those obtained using the BK parametrization, by as much as 10%, with significantly larger uncertainties obtained using the QA parametrization.

The form factor results from the BK fit are generally in good agreement with the form factors based on a global analysis including calculated TPE corrections [38], as well as some previous phenomenological extractions. For G_{Ep}, this is essentially because the polarization transfer data is assumed to be unaffected by TPE corrections and taken as a constraint in most of the extractions, while for G_{Mp}, the extraction is slightly more dependent on the detailed assumptions of the analyses. Using the BK parametrization, the TPE amplitude $a(Q^2)$ was extracted. The amplitude is on the few percent level, and increases in size with increasing Q^2. We find parametrize the TPE contribution and fit uncertainties as $a(Q^2) = (-0.0191 \pm 0.0014)\sqrt{Q^2} \pm 0.003$ for Q^2 from 1.5 to 4.0 (GeV/c)^2. We estimate that the uncertainties associated with the assumptions made in this extraction (no TPE correction to polarization data, linear of TPE contribution to the cross section, etc...), common to most of the extractions presented here, yield an uncertainty that is comperable to the quoted fit uncertainty, although these uncertainties are more likely to be strongly correlated with Q^2. Note that recent high-precision polarization measurements of $\mu_p G_{Ep}/G_{Mp}$ at low Q^2 [53–56], combined with expected results from comparison of positron and electron scattering, will significantly improve our knowledge of the TPE contributions at lower Q^2 values. However, at very low Q^2 values, the TPE contributions have significantly more impact on G_{Mp} [57, 58], which is more difficult to extract precisely in Rosenbluth measurements.

Note that the cross sections reported in Ref. [41] were determined by detecting recoiling protons, in contrast to all other measurements which detected the scattered electrons. The consistency of the extraction suggests that the approximations used to calculate standard radiative corrections, which yield very different corrections for these two cases, are reliable, although the quantitative comparison is limited by the precision of the electron detection measurements. A more extensive set of such measurements, covering $0.4 < Q^2 \lesssim 5$ (GeV/c)^2 is under analysis, and will allow for a much more detailed examination [56].

Finally, we compare extractions of the TPE contributions to the ratio of positron–proton and electron–proton scattering cross sections. We use these to make predictions for the higher Q^2 kinematics of the recently completed and ongoing measurements of $R^{e^+e^-}$. The lower Q^2 values enter the region where the present data are limited in their ability to extract TPE contributions based on the comparison of cross section and polarization measurements. The positron measurements will provide new information which can provide the first direct experimental evidence for TPE contributions at low-Q^2.

Acknowledgments

This work was supported by by Khalifa University of Science, Technology and Research and by the U. S. Department of Energy, Office of Nuclear Physics, under contract DE-AC02-06CH11357. We thank Mrs. Phyllis Burns and Dr. Nicolas Moore for reading the manuscript and making valuable comments and suggestions. We also thank the IT department at Khalifa University for their technical assistance.

[1] R. G. Sachs, Phys. Rev. **126**, 2256 (1962).
[2] M. N. Rosenbluth, Phys. Rev. **79**, 615 (1950).
[3] N. Dombey, Rev. Mod. Phys. **41**, 236 (1969).
[4] A. A. I. and M. P. Rekalo, Sov. J. Part. Nucl. **4**, 277 (1974).
[5] R. G. Arnold, C. E. Carlson, and F. Gross, Phys. Rev. C **23**, 363 (1981).
[6] J. Arrington, C. D. Roberts, and J. M. Zanotti (2006), arXiv:nucl-th/0611050.
[7] C. Perdrisat, V. Punjabi, and M. Vanderhaeghen, Prog. Part. Nucl. Phys. **59**, 694 (2007).
[8] O. Gayou et al., Phys. Rev. Lett. **88**, 092301 (2002).
[9] P. G. Blunden, W. Melnitchouk, and J. A. Tjon, Phys. Rev. Lett. **91**, 142304 (2003).
[10] P. G. Blunden, W. Melnitchouk, and J. A. Tjon, Phys. Rev. C **72**, 034612 (2005).
[11] S. Kondratyuk, P. G. Blunden, W. Melnitchouk, and J. A. Tjon, Phys. Rev. Lett. **95**, 172503 (2005).
[12] Y. C. Chen, A. Afanasev, S. J. Brodsky, C. E. Carlson, and M. Vanderhaeghen, Phys. Rev. Lett. **93**, 122301 (2004).
[13] D. Borisyuk and A. Kobushkin, Phys. Rev. C **74**, 065203 (2006).
[14] D. Borisyuk and A. Kobushkin, Phys. Rev. C **78**, 025208 (2008).
[15] P. A. M. Guichon and M. Vanderhaeghen, Phys. Rev. Lett. **91**, 142303 (2003).
[16] E. Tomasi-Gustafsson and G. I. Gakh, Phys. Rev. C **72**, 015209 (2005).
[17] V. Tvaskis et al., Phys. Rev. C **73**, 025206 (2006).
[18] Y.-C. Chen, C.-W. Kao, and S.-N. Yang, Phys.Lett. **B652**, 269 (2007).
[19] J. Arrington, Phys. Rev. C **71**, 015202 (2005).
[20] J. Guttmann et al., arXiv:1012.0564 (2011).
[21] I. A. Qattan and A. Alsaad, Phys. Rev. C **83**, 054307 (2011).
[22] D. Borisyuk and A. Kobushkin, Phys. Rev. D **83**, 057501 (2011).
[23] D. Borisyuk and A. Kobushkin, Phys. Rev. C **76**, 022201 (2007).
[24] C. E. Carlson and M. Vanderhaeghen, Ann. Rev. Nucl. Part. Sci. **57**, 171 (2007).
[25] J. Arrington, P. G. Blunden, and W. Melnitchouk, arXiv:1105.0951 (2011).
[26] M. Meziane et al., Phys. Rev. Lett. **106**, 132501 (2011).
[27] J. Mar et al., Phys. Rev. Lett. **21**, 482 (1968).
[28] I. A. Qattan, Ph.D. thesis, Northwestern University (2005), arXiv:nucl-ex/0610006.
[29] J. Arrington, Phys. Rev. C **69**, 032201(R) (2004).
[30] J. Arrington, Phys. Rev. C **69**, 022201(R) (2004).
[31] W. Alberico, S. M. Bilenky, C. Giunti, and K. M. Graczyk, Phys. Rev. C **79**, 065204 (2009).
[32] L. Andivahis et al., Phys. Rev. D **50**, 5491 (1994).
[33] J. J. Kelly, Phys. Rev. C **70**, 068202 (2004).
[34] W. Bartel, F.-W. Büsser, W.-R. Dix, R. Felst, D. Harms, H. Krehbiel, J. McElroy, J. Meyer, and G. Weber, Nucl. Phys. B **58**, 429 (1973).
[35] J. Litt et al., Phys. Lett. B **31**, 40 (1970).
[36] C. Berger, V. Burkert, G. Knop, B. Langenbeck, and K. Rith, Phys. Lett. B **35**, 87 (1971).
[37] W. Alberico, S. M. Bilenky, C. Giunti, and K. M. Graczyk, J. Phys. **G36**, 115009 (2009).
[38] J. Arrington, W. Melnitchouk, and J. A. Tjon, Phys. Rev. **C76**, 035205 (2007).
[39] R. C. Walker et al., Phys. Rev. D **49**, 5671 (1994).
[40] M. E. Christy et al., Phys. Rev. C **70**, 015206 (2004).
[41] I. A. Qattan et al., Phys. Rev. Lett. **94**, 142301 (2005).
[42] J. Arrington, Phys. Rev. C **68**, 034325 (2003).
[43] The cross section values used in this analysis are taken from http://www.jlab.org/resdata.
[44] D. Borisyuk and A. Kobushkin, Phys. Rev. C **75**, 038202 (2007).
[45] J. Arrington and I. Sick, Phys. Rev. C **70**, 028203 (2004).
[46] A. V. Afanasev, S. J. Brodsky, C. E. Carlson, Y.-C. Chen, and M. Vanderhaeghen, Phys. Rev. D **72**, 013008 (2005).
[47] J. Arrington, D. M. Nikolenko, et al., Proposal for positron measurement at VEPP-3, nucl-ex/0408020.
[48] D. M. Nikolenco et al., Phys. Atom. Nucl. **73**, 1322 (2010).
[49] D. M. Nikolenco et al., PoS ICHEP2010 p. 164 (2010).
[50] W. Brooks et al., Jefferson lab experiment E07-005.
[51] M. Kohl, AIP Conf. Proc. **1160**, 19 (2009).
[52] D. Borisyuk and A. Kobushkin, Phys. Rev. D **79**, 034001 (2009).
[53] J. C. Bernauer et al., Phys. Rev. Lett. **105**, 242001 (2010).
[54] X. Zhan et al. (2011), arXiv:1108.4441.
[55] G. Ron et al. (2011), arXiv:1103.5784.
[56] J. Arrington et al., Jefferson Lab experiment E05-017.
[57] J. Arrington (2011), arXiv:1108.3058.
[58] J. C. Bernauer et al. (2011), arXiv:1108.3533.